Papers

Colorectal tumours and pit pattern

S Kudo, S Hirota, T Nakajima, S Hosobe, H Kusaka, T Kobayashi, M Himori, A Yagyuu

The Department of Gastroenterology, Akita Red Cross Hospital, 1-4-36 Nakadouri Akita City, Japan
S Kudo
S Hirota
T Nakajima
S Hosobe
H Kusaka
T Kobayashi
M Himori
A Yagyuu
Correspondence to:
Dr S Hirota
Accepted for publication
24 March 1994

Abstract

Aims—To investigate the morphological and histopathological associations between an individual pit seen on stereomicroscopy or magnifying colonoscopy and an individual crypt seen in histological sections; and to examine these associations in colorectal tumours.

Methods—Fourteen thousand and twenty three cases were examined by colonoscope at Akita Red Cross Hospital. The surface mucosal pits of the lesions were observed using a magnifying endoscope in vivo and the pits of the extracted specimens were observed in vitro using a stereo microscope. Histological diagnoses were determined by light microscopy: the pit patterns in 100 glands were analysed.

Results—Pit pattern was classified into seven principal types: (1) normal round pit; (2) small round pit; (3) small asteroid pit; (4) large asteroid pit; (5) oval pit; (6) gyrus-like pit; and (7) non-pit. There was a correlation between pit pattern and the structure of the underlying crypt or gland. Furthermore, there was an association between pit pattern and the histology of the cells in the gland. Macroscopically, types 3, 4, 5, and 6 were common in protruding lesions. Type 2 was common in depressed lesions. The non-pit pattern was recognised in both. The depressed lesions had invaded the deeper layers more rapidly than protruding lesions.

Conclusions—There were associations between individual pits and crypts. The branching carcinoma gland is thought to be the result of malignant transformation of the adenoma gland. The straight carcinoma gland is thought to result from the normal gland becoming malignant. The gland of the small round pit is thought to change from normal to the straight carcinoma gland via malignant transformation.

(*J Clin Pathol* 1994;47:880–885)

We used a magnifying endoscope with a zoom range from one to 100 magnification (Olympus, Tokyo, Japan), to observe pit patterns (the shape of the opening of a colorectal crypt) on the surface of normal bowel and of colorectal tumours in vivo. The pit patterns of specimens extracted from the colorectum by

Table 1 Classification of pit pattern

	Normal round pit	Small round pit	Small asteroid pit	Large asteroid pit	Oval pit	Gyrus-like pit	Non-pit	
Mean length	361·56	243·12	432·56	485·24	> 500	> 500	180·52	> 500 *
Branching number	0	0	0	2-3	2-3	4-6	0	2-6 *
Mean major axis								
surface	104·79	53·06	132·43	192·21	257·06	726·46	*	* *
100 μm	87·24	68·27	105·24	186·42	212·54	515·42	50·42	682·23 *
200 μm	85·46	48·33	102·54	121·25	138·42	505·64	50·32	582·48 *
300 μm	84·76	44·41	92·48	116·76	153·33	483·72		502·13 *
400 μm	85·76		91·36	106·72	147·51	313·34		* *
Mean distance								
surface	46·33	23·18	36·62	43·27	20·39	50·34	*	* *
100 μm	54·14	23·47	25·81	23·12	14·17	32·41	42·15	18·26 *
200 μm	78·63	43·63	18·33	18·14	10·21	28·21	40·23	12·54 *
300 μm	78·43	43·65	15·41	15·41	13·62	21·65		10·25 *
400 μm	80·47		15·21	14·28	13·24	19·27		*
Mean area								
surface	8661·96	2689·56	11979·94	18815·23	28792·96	85053·28	*	* *
100 μm	5682·36	3829·84	8409·31	9025·59	18877·51	69080·52	1962·55	10990·38 *
200 μm	5679·45	2195·13	7590·87	7604·69	15655·84	68687·51	1256·22	1923·25 *
300 μm	5549·55	1838·21	6260·38	6384·67	14306·63	40196·94		1513·74 *
400 μm	5379·48		4297·86	5863·79	12860·92	25601·87		* *
Mean total area								
surface				18815·23	28792·96	85053·28		* *
100 μm				17328·45	26877·12	80234·15		10990·38 *
200 μm				17212·52	20331·96	69080·41		9615·45 *
300 μm				17002·46	15655·84	65724·72		8842·28 *
400 μm				15826·46	14306·63	63894·18		*
Histology	Normal gland	borderline or carcinoma gland	Hyperplastic gland	Serrated adenoma gland	Adenoma gland	Tubulovillous gland	Carcinoma gland	

Length μm; area μm²; *the layer of the fibromatous tissues or non-structural glands.

Figure 1   A Stereo-microscopic view of normal round pit pattern. The round shape pits are arranged at almost regular intervals (Carazzi's haematoxylin stain).B Microscopic vertical view with haematoxylin and eosin. The glands are straight, non-branching.C Surface macroscopic horizontal view. A round-shaped gland composed of goblet cells can be seen.D Microscopic horizontal view at 200 µm depth. A round-shaped gland can be seen.
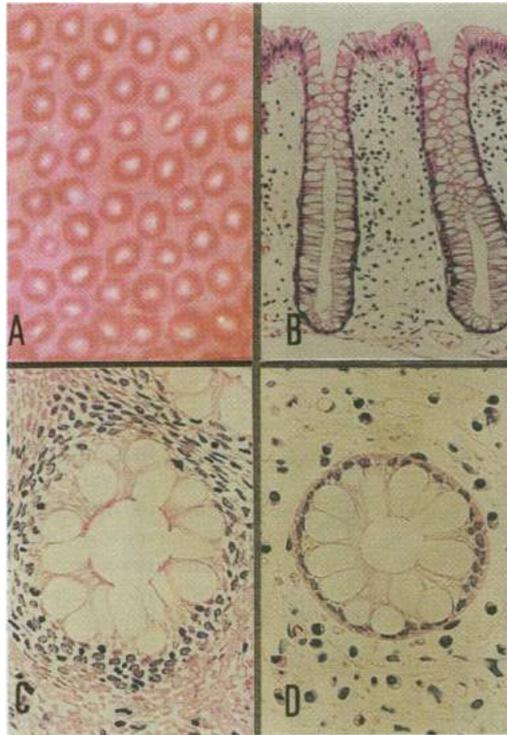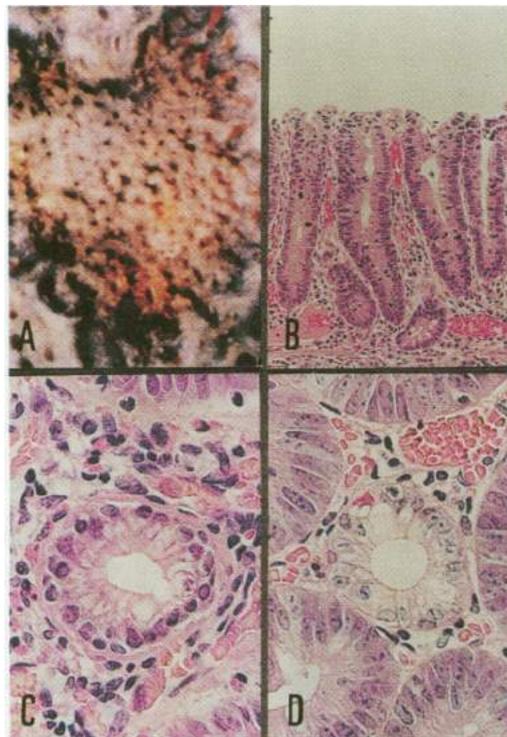

Figure 2   A Stereo-microscopic view of small round pit pattern. The small round-shaped pits can be seen in dense groups (Carazzi's haematoxylin). B Microscopic vertical view: the glands are straight, non-branching (haematoxylin and eosin).C Surface microscopic horizontal view. A small round shaped gland can be seen.D Microscopic horizontal view at 200 µm depth. A small round shaped gland, composed of borderline malignant cells or carcinoma cells and surrounded by the adenoma glands with the oval pit can be seen.
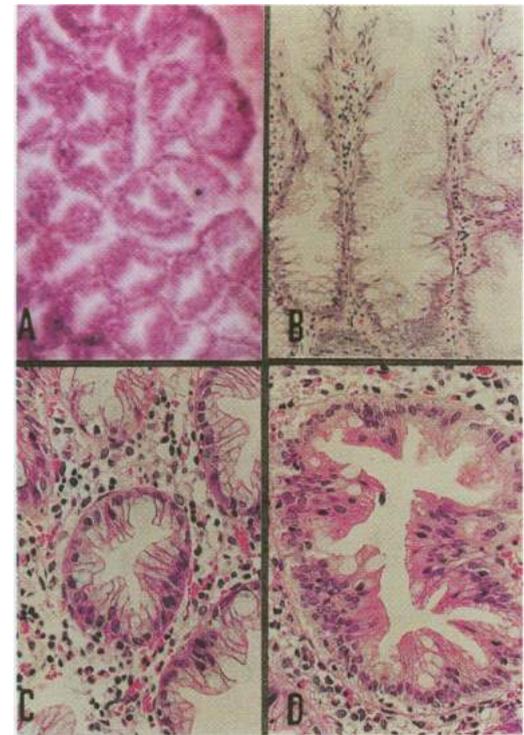

Figure 3   A Small asteroid pit pattern. The asteroid shape pits are arranged at almost regular intervals (Carazzi's haematoxylin stain).B Microscopic vertical view with haematoxylin-eosin stain. The glands of the small asteroid pit are straight, non-branching, and winding with the hyperplastic change (haematoxylin and eosin).C Surface microscopic horizontal view. A small asteroid shaped gland with hyperplastic change can be seen.D Surface microscopic horizontal view. A large asteroid shaped gland with the adenomatous change can be seen. This gland is branching.
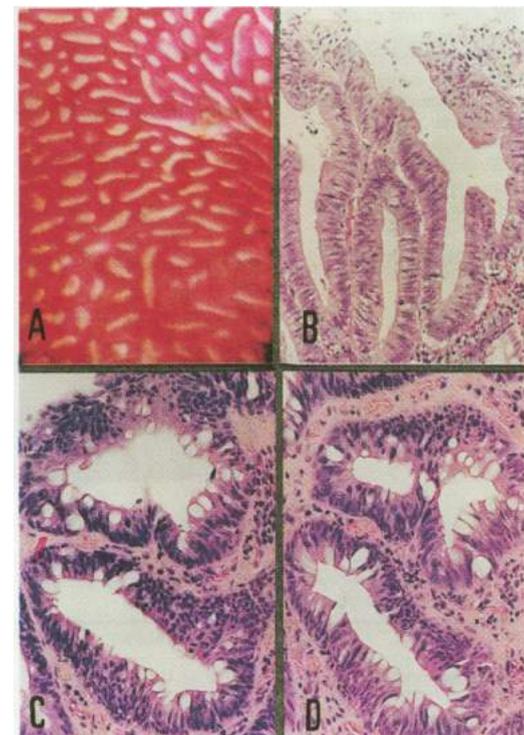

Figure 4   A Oval pit pattern. The oval or the long and slender shaped pits are arranged at irregular intervals (Carazzi's haematoxylin).B Vertical view: the glands are branching (haematoxylin and eosin).C Surface microscopic horizontal view. The oval shaped glands can be seen.D Microscopic horizontal view at 50 µm depth. A gland divides from one gland into two smaller glands.

polypectomy, endoscopic mucosal resection (EMR), and surgery, used to be examined using a stereo microscope (Olympus, Tokyo, Japan). In this study we examined the correlation between one pit and one gland from a morphological and histopathological point of view. The pattern of development of neoplasia was correlated from these results.

Methods
Between 1987 and 1993, 14023 patients

Figure 5 A Gyrus-like pit pattern. The branch-like or gyrus-like shape pits are arranged at irregular intervals (Carazzi's haematoxylin).B Microscopic vertical view: one gland divides into several glands (haematoxylin and eosin).C Surface microscopic horizontal view. Branch-like or gyrus-like shape glands can be seen.D Microscopic horizontal view at 80 μm depth. The glands branch out into smaller glands.
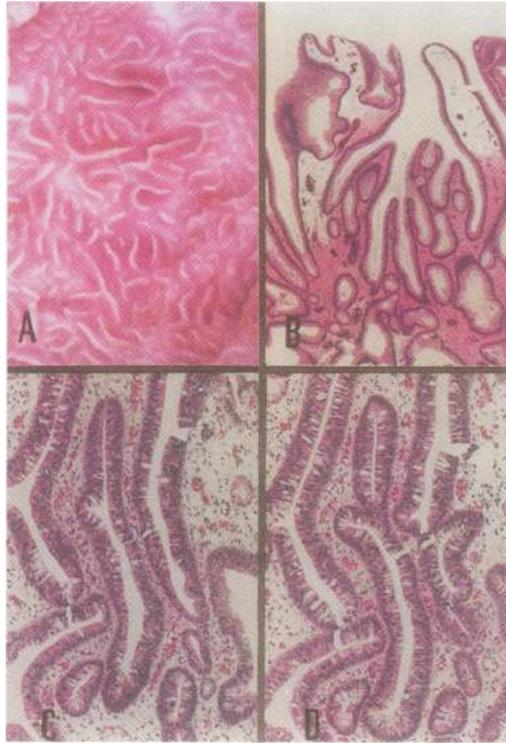
Figure 6 A Non-pit pattern. Non-structural surface is recognized. No pits can be seen (Carazzi's haematoxylin stain).B Microscopic view of vertical axis (haematoxylin and eosin). Under the fibromatous tissues, a straight, non-branching gland composed of carcinoma cells can be seen. This gland exists in the mucosal portion of the carcinoma lesion which has invaded the submucosal layer.C Microscopic view of vertical axis. A branching gland composed of carcinoma cells is evident.D Microscopic view of vertical axis. Fibromatous tissues and non-structural carcinoma cells or glands can be mainly seen.
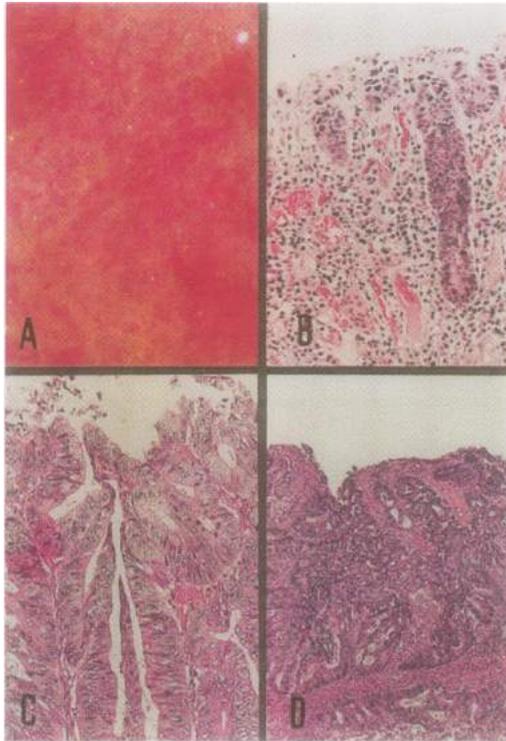
(8400 male cases; 5623 female cases, aged from 6 to 85 years old) were investigated by colonoscopy at Akita Red Cross Hospital. Of these, 4329 patients had undergone polypectomy, 1413 endoscopic mucosal resection (EMR), and 237 were surgical cases. Histological diagnoses were determined according to the World Health Organisation (WHO) criteria.[1]

Specimens were fixed in 20% formaldehyde solutions. For light stereo microscopy, the specimens were stained with Carazzi's haematoxylin. There were then embedded in paraffin wax. Each specimen was cut in half: one half was cut into 3 μm thick sections on the vertical axis, the other half into 3 μm thick sections on the horizontal axis from mucosal surface to muscularis mucosae, and stained with haematoxylin and eosin.

The pits seen on magnifying colonoscopy (×60) and stereo microscopy (×60) were classified into normal, small round, small asteroid, large asteroid, oval, gyrus-like pits, and absent. One hundred crypts of each pit pattern were analysed. Their diameter and area were measured using computer analysis. Submucosal tumours and squamous epithelial origin tumours were excluded.

Results

Seven types of pit pattern were classified (table 1). (1) *Normal round pit*: The crypts were all straight, non-branching. The cells looked histopathologically normal. These crypts were diagnosed as normal (100%). Macroscopically, they were seen on normal mucosa (100%) (figs 1 A-D). (2) *Small round pit*: The crypts were all straight and non-branching. Histopathologically, the cells showed borderline malignant or carcinomatous change. These crypts were diagnosed as borderline malignant (72%) or adenocarcinoma (28%). Macroscopically, they were seen more often in depressed lesions than in protruding lesions (table 2, figs 2 A-D). Beneath these crypts, isolated borderline malignant or carcinoma glands which were not apparently connected with the surface were often seen. (3) *Small asteroid pit*: The crypts were all straight, non-branching. Histopathologically, the cells showed slight swelling but no atypia. These glands were diagnosed as hyperplastic (100%). Macroscopically, they were seen in protruding lesions (100%) (figs 3 A-C and figs 7 A, B). (4) *Large asteroid pit*: These crypts were all branching. They started to branch at a depth of 30–100 μm, then branched repeatedly, becoming smaller. The crypts were absent at a depth of over 500 μm. Histopathologically, the cells were slightly swollen and mildly atypical. These crypts were diagnosed as hyperplastic or as serrated adenoma. Macroscopically, they were seen in protruding lesions (100%) (fig 3 D). (5) *Oval pit*: These crypts were all branching. They began to branch at a depth of 30–100 μm, then branched repeatedly with several round crypts. At greater depths, the glands were absent. Histopathologically, the cells looked

Table 2   Morphological forms and pit patterns

	Small round pit	Oval pit	Gyrus pit	Non-pit
Protruding lesion	215 (13·6%)	1021 (64·7%)	325 (20·6%)	18 (1·1%)
Depressed lesion	61 (64·9%)	22 (23·4%)	0 (0·0%)	11 (11·7%)

Table 3   Size and form of submucosal invasive carcinoma

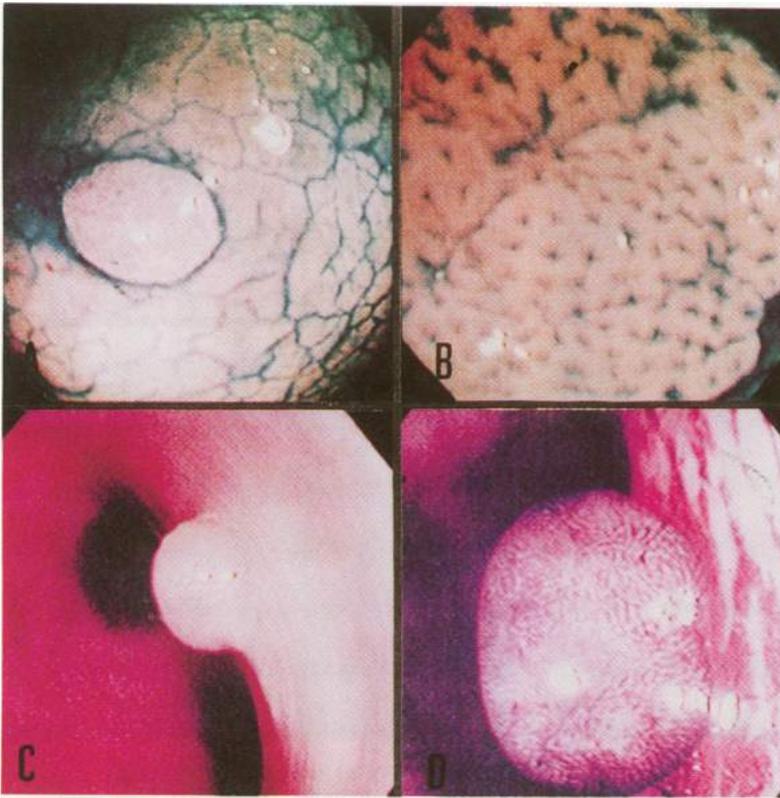|	5 mm	10 mm	11 mm and over
Protruding lesion	3 (3·3%)	23 (25·0%)	66 (71·7%)
Depressed lesion	8 (42·1%)	9 (47·4%)	2 (10·5%)

Figure 7   A Usual endoscopic view using a contrast method. The protruding lesion is evident. B Magnifying endoscopic view using a contrast method. Asteroid pits can be seen. This lesion was diagnosed as hyperplastic polyp. C Usual endoscopic view of protruding lesion. D Magnifying endoscopic view, using a contrast method and showing oval pits. This lesion was diagnosed as adenomatous polyp.
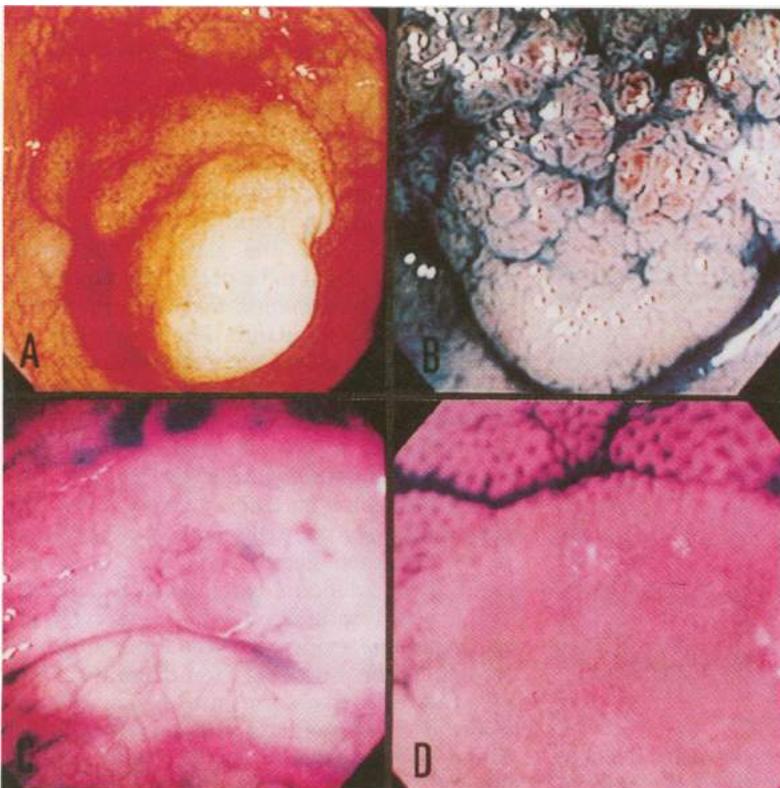

Figure 8   A Usual endoscopic view of protruding lesion. B Magnifying endoscopic view using a contrast method showing gyrus-like pits. This lesion was diagnosed as tubulovillous adenoma polyp. C Usual endoscopic view using a contrast method showing a depressed lesion. D Magnifying endoscopic view using a contrast method, showing a non-pit pattern. Around the non-pit lesion, normal round pits can be seen. This lesion was diagnosed as submucosal invasive carcinoma.

moderately atypical. These glands were diagnosed as adenoma (100%). Macroscopically, they were more common in protruding than in depressed lesions (table 2, figs 4 A-D, figs 7 C, D). (6) *Gyrus-like pit:* The giant crypts were all branching. They began to branch at a depth of 50–100 μm, branching repeatedly with several round or oval shaped crypts. Histopathologically, the cells were moderately atypical. These crypts were diagnosed as adenoma (100%), and were found in almost all the tubulovillous adenomas. Macroscopically, they were more common in protruding lesions (100%) (table 2, figs 5 A-D, figs 8 A, B). A gyrus-like pit seemed to result in a growth of an oval pit. (7) *Non-pit:* These comprised a layer of fibromatous tissues or non-structural glands from the surface to 30-80 μm in depth (fig 6 A). Beneath that layer, the crypts were evident. The non-pit category was classified into three further subtypes: straight, nonbranching (fig 6 B); and branching crypts at a depth of 80–100 μm, branching repeatedly and changing to the several crypts with abundant stroma. At greater depths, the crypts were mixed with stroma and disappeared (fig 6 C). The third subtype was undifferentiated adenocarcinoma or a mixture of stroma and carcinoma glands (fig 6 D). In each case, the cells contained malignant cells on histopathology. These glands were diagnosed as adenocarcinoma glands (100%) which had invaded the submucosal or deeper layers. The following abbreviations were used in this study: type I, normal round pit; type II, small and large asteroid pits; type IIIs, small round pit; type IIIL, oval pit; type IV, gyrus-like pit; and type V, non-pit pattern (Kudo's classification).

Macroscopically, they were seen on both protruding lesions and depressed lesions (table 2, figs 8 C, D).

Discussion

We analysed the association between an individual pit and an individual gland in each type of pit pattern. As colorectal carcinomas originate from the mucosal surface, it is not appropriate to diagnose cell atypia and structural atypia in sections of the submucosal or deeper layers. To investigate the spontaneous development of colorectal carcinomas, it is better to examine the mucosal layer, paying attention to the glands which open to the surface. We therefore observed and analysed mucosal lesions. We consider that the noteworthy points concerning the colorectal tumours were as follows:

Depressed lesions are thought to invade more rapidly than protruding lesions. In depressed lesions the small round pit was common (tables 2 and 3). Depressed lesions composed of crypts related to small round pits are thought to be the most important.

The straight carcinoma gland is thought to result from the normal gland becoming malignant. It is the de novo carcinoma gland. In this gland structural atypia is scarcely evident, so cell atypia is the most important feature for
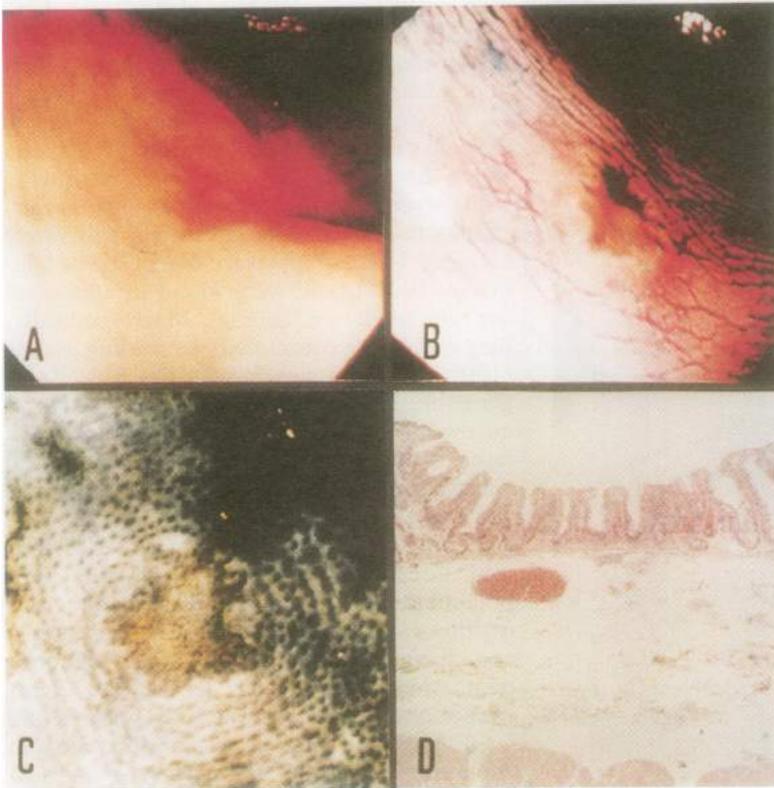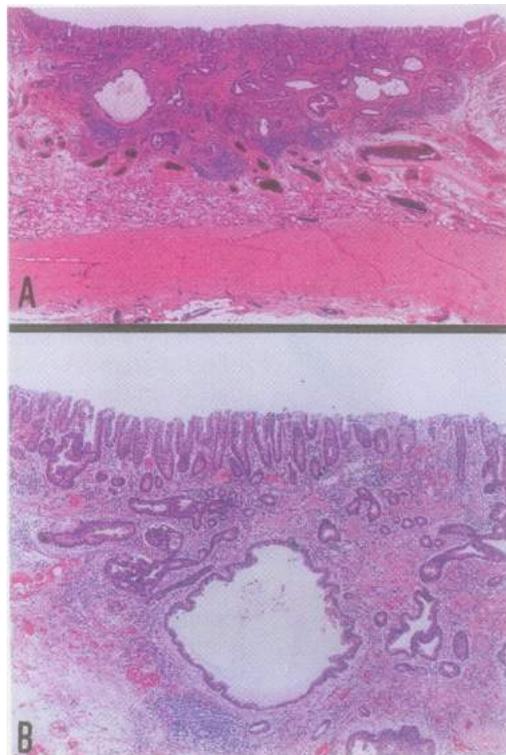
Figure 9 A Usual endoscopic view of depressed lesion. B Usual endoscopic view using a contrast method. C Stereo microscopic view (Carazzi's haematoxylin) of small round pits. Normal round pits can be seen around the small round pits. D Microscopic view of vertical axis. The straight glands are densely arranged. These glands were diagnosed as borderline malignant.
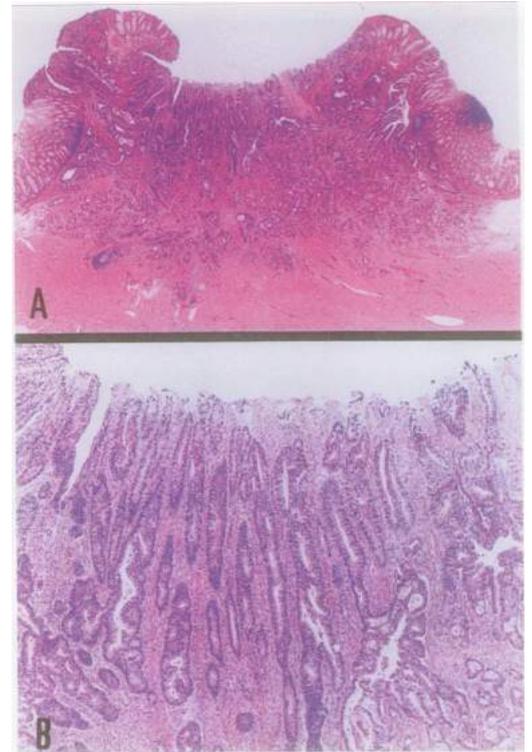

Figure 11 A, B Microscopic view of vertical axis (haematoxylin and eosin). The depressed lesion was diagnosed as advanced carcinoma (9 × 9 mm). Under the straight carcinoma glands with non-pit lesions (covered with fibromatous tissue), the carcinoma glands show independent growth, loss of polarity and bearing, and progression in all directions. This lesion is thought to be the de novo carcinoma lesion.

Figure 10 A, B Microscopic view of vertical axis (haematoxylin and eosin). The depressed lesion was diagnosed as submucosal invasive carcinoma (7 × 7 mm). Under the straight carcinoma glands with the small round pit or non-pit lesions, the carcinoma glands show independent growth, loss of polarity and bearing, and progression in all directions. This lesion is thought to be the start of the de novo carcinoma glands.

diagnosis. Firstly, the normal cells become malignant at the point at which the normal gland begins to divide (the bottom of gland). As a result, cell turnover from the bottom to the surface becomes slow which in turn slows growth of the gland. The gland is therefore shorter and smaller than neighbouring normal glands. Finally, the gland of the small round pit appears. If blood circulation is poor, the surface mucosal layer easily develops necrosis. Additionally, if the carcinoma cells at the bottom of gland destroy gland formation and grow independently, invading the deeper layers, poor blood circulation rapidly occurs. As a result of necrosis of the surface mucosa, the straight carcinoma gland with the non-pit appears. Above all, the gland of the small round pit is thought to be part of the process of malignant transformation from normal to the straight carcinoma gland. The borderline de novo malignant gland has a straight structure and is short in length. It easily invades into the deeper layers independently and leads to surface necrosis. It has the highest malignant potential histopathologically (figs 9–11).

The branching carcinoma gland is thought to be a result of the malignant transformation of the adenoma gland. It is the carcinoma gland of the adenoma-carcinoma sequence.[2-4] In this gland both architectural and cytological atypia are evident. Cytological atypia is thought to be important for diagnosis. The adenoma cells transform into malignant cells at the division point of the adenoma gland (about 100 μm from the surface) and the carcinoma cells replace the adenoma gland. As the area and the volume of the adenoma glands are greater than that of the normal glands, it takes quite a long time to replace the adenoma glands with the carcinoma glands. As poor blood circulation and surface necrosis

rarely occur, the non-pit pattern is not seen until the carcinoma invades extensively into the submucosal layer or the deeper layer. Accordingly, there are quite a few focal carcinoma cells and glands in the adenoma lesions. Consequently, the branching gland has lower malignant potential than that of the small round pit.

Poorly differentiated cells (arising either de novo or of adenoma origin) rapidly invade the deeper layers early without forming clear glandular structures. The non-pit pattern appears early.

The carcinoma cells and glands which have invaded into the deeper layer lose their polarity and progress in all directions. Various cytological and architectural atypia can be seen.

The glands of the small round pit sometimes coexist with the glands of the oval or gyrus-like pit. This lesion is thought to transform quickly into de novo carcinoma glands. Furthermore, if adenoma glands become malignant de novo carcinoma glands and carcinoma glands of adenoma origin can coexist.

CLINICAL CORRELATIONS

Clinically, we can diagnose neoplastic lesions and decide on treatment by observing the pit patterns using the magnifying endoscope in vivo. The normal round pit is seen in both depressed lesions and protruding lesions. Except for carcinoid tumours, they are usually simply followed up. In asteroid pits, the lesions are usually followed up. The highly protruding lesions with large asteroid pits are treated by polypectomy or EMR. In lesions with small round pits, oval pits, or gyrus-like pits, the lesions must be resected by polypectomy or EMR (especially those with small round pits). In non-pit lesions, protruding lesions are usually resected by polypectomy or EMR. Whether follow up or additional surgery is decided on depends on the histopathological diagnosis. Depressed lesions are usually surgically resected.

The depressed lesion with the small round pit is the most important. The crypt of the small round pit shows a straight structure and has the highest malignant potential. The straight carcinoma gland is the de novo carcinoma gland. The gland of the small round pit is thought to be an intermediate stage of malignant transformation of the normal gland to the straight carcinoma gland.

1 Morson BC, Sobin LH. Histological typing of intestinal tumours. Geneva: World Health Organisation, 1976.
2 Bussey HJR. Familial polyposis coli. Baltimore: Johns Hopkins University Press, 1975:47–58.
3 Helwig EB. Adenomas and the pathogenesis of cancer of the colon and rectum. Dis Colon Rectum 1959;2:5–17.
4 Hill MJ, Morson BC, Bussey HJR. Aetiology and adenocarcinoma sequence in large bowel. Lancet 1978;i: 245–7.